Water Hammer in Offloading Systems: Contribution of Detailed Modeling to Design and Safety

B. Pierre, SPE, and **J.S. Gudmundsson,** SPE, Norwegian University of Science and Technology

Summary

The second-largest oil spillage in Norwegian petroleum history occurred on 12 December 2007 when the Statfjord A offloading system ruptured. Results of numerical simulations of pressure transients in the offloading system are presented. Of particular interest is the influence of acoustic properties of pipeline sections on propagation of pressure transients. The damaged-offloading-system geometry and characteristics, as well as the acoustic properties, are described. The paper describes numerical simulations of pressure transients in the offloading pipeline. The paper shows how detailed modeling and accurate estimation of acoustic velocities influence local maximum increases in pressure in an offloading system.

Introduction

Hydrocarbon-transport pipelines are subject to rapid pressure transients in the form of water-hammer events. Rapid pressure transients can arise when quick-acting valves are suddenly actuated or after pump failure. Consequences of rapid pressure transients in hydrocarbon-transport pipelines range from operational damages, such as leakages (Moura et al. 2004; Wang et al. 2004), to pipe rupture (Misiunas et al. 2005). Therefore, rapid pressure transients need to be predicted accurately in hydrocarbon-transport pipelines in order to prevent damages.

Offloading systems typically consist of many individual pipes and pieces of equipment such as pumps and valves. Calculations and modeling of rapid-pressure-transient events need to account for all the sections and pieces of equipment included in the system.

The Statfjord A offloading system is a 2808-m-long oil-transport system made of 40 pipes, one pump, and one shut-in valve (Norwegian Coastal Administration 2008). The offloading system connects a storage tank located at the base of a production platform to a single-path coupler (shut-in valve) located on a shuttle tanker. The Statfjord A offloading system ruptured on 12 December 2007 because of a rapid-pressure-transient event generated by sudden actuation of the shut-in valve (Pierre and Gudmundsson 2008).

Rupture of the Statfjord A offloading system caused 4400 m^3 of oil to be pumped into the sea, thus generating the second-largest spillage in the history of oil activities in Norway. Predictions of rapid pressure transients need to be accurate in order to prevent future accidents.

Predictions of rapid pressure transients produce different results, depending on whether all the sections are considered or not. Of particular interest is the influence of the many pipe geometrical and material properties on the local maximum pressure reached during superposition of pressure waves.

Modeling Equations

Pressure transients propagate in oil-filled offloading systems in the form of pressure waves. Offloading systems are typically tens of inches in diameter and several kilometers in length, hence the use of 1D modeling. Propagation of pressure waves can be modeled using mass- and momentum-conservation equations. Maximum flow velocities of oil in offloading systems typically range from 4 to 8 m/s, whereas acoustic velocities in oil-filled offloading systems typically range from 700 to 1200 m/s, giving low-Mach-number flows (Ma = u/a). 1D mass- and momentum-conservation equations can then be expressed in a simplified conservative form, respectively, by (Ghidaoui et al. 2005)

$$\frac{\partial p}{\partial t}+\frac{\partial}{\partial x}\left(\rho a^2 u\right)=0$$

$$\rho\frac{\partial u}{\partial t}+\frac{\partial p}{\partial x}=\frac{-f}{2}\rho u\left|u\right|+F, \quad (1)$$

where p is pressure, u is flow velocity, a is acoustic velocity, ρ is density, f is steady friction factor, and F is external forces such as gravity. Steady friction and external forces define a source term. Source-term modeling represents mechanisms responsible for pressure-wave attenuation in terms of damping of pressure amplitudes and smoothing of pressure waveforms. Steady frictional pressure drop is the only attenuation mechanism herein considered. Other mechanisms, including unsteady friction or pipeline viscoelasticity, are neglected because of the uncertainty of their validity (Pierre and Gudmundsson 2009). The present study is comparative, and the omission of accurate attenuation mechanisms corresponds to the study of a worst-case scenario.

Pressure transients propagate in fluid-filled pipelines at the speed of sound, a. Speeds of sound, or acoustic velocities, depend on fluid elastic properties, density, and isothermal compressibility, K_T, and pipeline characteristics such as diameter, d, wall thickness, e, and wall-material Young's modulus of elasticity, Y. The acoustic velocity in a fluid-filled pipeline can be expressed by (Wylie et al. 1993):

$$a=\sqrt{\frac{1}{\rho\left(K_T+\frac{d}{Ye}\sigma_\mu\right)}}, \quad (2)$$

where σ_μ represents a structure coefficient that depends on pipeline-wall-material Poisson's ratio, μ; pipeline dimensions; and anchoring. Structure coefficients are listed in **Table 1** for completeness (Wylie et al. 1993). Offloading systems are anchored upstream and downstream to a storage tank and to a shuttle tanker, respectively. In addition, offloading systems are flexible structures. Thus, structure coefficients for calculations of acoustic velocities in oil-filled offloading pipelines correspond to anchoring at both ends with expansion joints (Table 1).

Acoustic velocities in oil-filled thin- and thick-walled steel and flexible pipelines are illustrated in **Fig. 1.** Acoustic-velocities calculations are based on typical oil density and isothermal compressibility, 760 kg/m^3 and 1.98 10^{-9} Pa^{-1}, respectively (McCain 1990); steel and steel-reinforced-rubber Young's modulus of elasticity, 200 10^9 Pa and 1.9 10^9 Pa, respectively; and steel and steel-reinforced-rubber Poisson's ratio, μ, 0.3 and 0.5, respectively (Cheremisinoff 1996).

Calculated acoustic velocities increase with wall-thickness/diameter ratios, e/d. Acoustic velocities in oil-filled flexible thin-walled

This paper (SPE 134140) was accepted for presentation at the SPE Annual Technical Conference and Exhibition, Florence, Italy, 19–22 September 2010, and revised for publication. Original manuscript received 1 June 2010. Revised manuscript received 20 October 2010. Paper peer approved 8 November 2010.

TABLE 1—STRUCTURE COEFFICIENTS σ_μ (WYLIE ET AL. 1993)		
Anchoring	Thin-Walled Pipeline	Thick-Walled Pipeline
Anchoring at Upstream End Only	$1-\frac{\mu}{2}$	$\frac{2e}{d}(1+\mu)+\frac{d}{d+e}\left(1-\frac{\mu}{2}\right)$
Anchored at Both End Against Axial Movement	$1-\mu^2$	$\frac{2e}{d}(1+\mu)+\frac{d}{d+e}(1-\mu^2)$
Anchored at Both Ends With Expansion Joints	1	$\frac{2e}{d}(1+\mu)+\frac{d}{d+e}$

pipelines increase from 215.6 to 324.4 to 392.1 m/s, for wall-thickness/diameter ratios of 2, 5, and 8%, respectively. Acoustic velocities in oil-filled steel pipelines increase from 766.7 to 793.8 to 801 m/s, for wall-thickness/diameter ratios of 2, 5, and 8%, respectively. Acoustic velocities calculated in oil-filled steel pipelines are independent of the nature of the wall (thin or thick).

Calculated acoustic velocities in oil-filled thin-walled flexible pipelines are greater than those in thick-walled flexible pipelines. At 5% wall-thickness/diameter ratio, calculated acoustic velocities in oil-filled thin-walled and thick-walled flexible pipelines are 324.4 and 311.2 m/s, respectively. Acoustic velocities calculated in oil-filled flexible pipelines should include the thick-walled structure coefficient for wall-thickness/diameter ratios greater than 5% (d/e = 20) (Watters 1984).

Changes in acoustic velocities create acoustic interfaces where pressure waves reflect and transmit. Changes in acoustic velocities can result from changes in fluid properties, density or fluid compressibility, or pipe characteristics, dimensions, or materials. Acoustic reflection and transmission coefficients can be expressed, respectively, by (Pain 1993):

$$R_{1\to2}=\frac{z_2-z_1}{z_2+z_1} \quad \text{(3)}$$

$$T_{1\to2}=\frac{2z_2}{z_2+z_1}, \quad \text{(4)}$$

where z represents acoustic impedance (z = ρa), Subscript 1 is medium upstream of the acoustic interface, and Subscript 2 is medium downstream of the acoustic interface.

Test Cases

Propagation of pressure transients in the form of a water hammer is investigated in the Statfjord offloading system that connects a storage tank at the base of the Statfjord A platform to a shuttle tanker 2807.75 m away. The Statfjord offloading system includes a pumping station that induces flow from the platform storage tank into the pipeline and a shut-in valve between the pipeline and the tanker. Sudden actuation of the shut-in valve generates a pressure wave in the form of a water hammer that propagates in the offloading system.

The Statfjord offloading system is composed of a succession of pipes of different dimensions and materials. Pipe materials used in the Statfjord off-loading system are steel and reinforced rubber. Young's modulus and Poisson's ratio for steel are 200×10^9 Pa and 0.3, respectively (Cheremisinoff 1996). Young's modulus and Poisson's ratio for rubber are 0.1×10^9 Pa and 0.5, respectively (Cheremisinoff 1996). However, steel reinforcements increase axial stiffness, and thus the Young's modulus. A Young's modulus of 1.9×10^9 Pa is assumed for steel-reinforced rubber pipes.

Pipe dimensions vary in wall thickness, length, and diameter. Wall thickness for steel and flexible pipes are 0.02 and 0.08 m, respectively, in the Statfjord offloading system. A complete description of the Statfjord offloading system, partially represented in **Fig. 2,** is given in **Table 2.** Pipes before a flange located 2716.25 m from the pump are 0.482 m in diameter, whereas pipes downstream of the flange are 0.508 m in diameter. Two swivels are located along the offloading system at 2625.25 and 2763.25 m.

An approximate oil composition at 5°C and 30 bara is given in **Table 3.** Density and viscosity obtained using the Peng-Robinson equation of state included in HYSYS are 737.3 kg/m^3 and 0.65 cp, respectively. The corresponding oil isothermal compressibility was then 2.02 10^{-9} Pa^{-1}. Acoustic velocities in steel and reinforced rubber

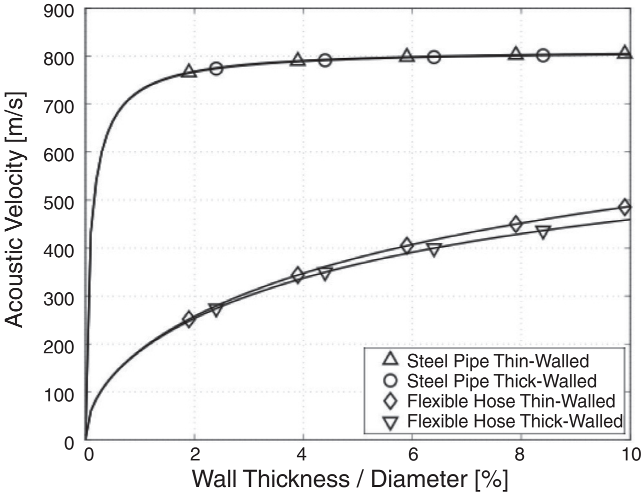

Fig. 1—Comparison of acoustic velocities in thin-walled and thick-walled oil-filled steel and flexible pipelines.

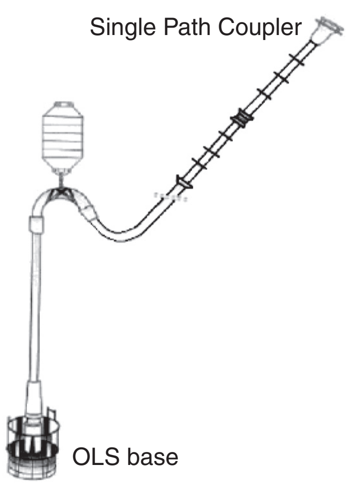

Fig. 2—Partial representation of Statfjord offloading system, between first swivel and shut-in valve.

TABLE 2—DETAILED DESCRIPTION OF STATFJORD OFFLOADING SYSTEM											
	L (m)	Material	x (m)		L (m)	Material	x (m)		L (m)	Material	x (m)
Valve				Swivel	2.00	Steel	2763.25		0.75	Steel	2715.25
	0.75	Steel	2807.75		0.75	Steel	2761.25		78.50	Rubber	2714.50
	0.75	Steel	2807.00		9.75	Rubber	2760.50		0.75	Steel	2636.00
	8.50	Rubber	2806.25		0.75	Steel	2750.75		10.00	Steel	2635.25
	0.75	Steel	2797.75		0.75	Steel	2750.00	Swivel	1.00	Steel	2625.25
	0.75	Steel	2797.00		9.75	Rubber	2749.25		0.75	Steel	2624.25
	9.75	Rubber	2796.25		0.75	Steel	2739.50		78.50	Rubber	2623.50
	0.75	Steel	2786.50		0.75	Steel	2738.75		0.75	Steel	2545.00
	0.75	Steel	2785.75		9.75	Rubber	2738.00		0.75	Steel	2544.25
	9.75	Rubber	2785.00		0.75	Steel	2728.25		26.75	Rubber	2543.50
	0.75	Steel	2775.25		0.75	Steel	2727.50		0.75	Steel	2516.75
	0.75	Steel	2774.50		9.75	Rubber	2726.75		2235.00	Steel	2516.00
	9.75	Rubber	2773.75		0.75	Steel	2717.00		281.00	Steel	281.00
	0.75	Steel	2764.00	Flange	1.00	Steel	2716.25	Pump			0

TABLE 3—APPROXIMATE STATFJORD OIL MOLAR COMPOSITION AT 5°C, 30 BARA					
Component	% mol	Component	% mol	Component	% mol
N_2	0.04	nC_4	6.25	C_9	5.61
CO_2	0.19	iC_5	2.09	C_{10}	4.43
C_1	9.32	nC_5	3.32	C_{11}	3.57
C_2	6.25	C_6	5.33	C_{12}	27.19
C_3	10.27	C_7	7.44		
iC_4	1.81	C_8	6.87		

pipes are listed in **Table 4** for diameters used in the offloading system and using thin-walled and thick-walled expressions of the acoustic velocity.

Three offloading systems are herein considered that correspond to different levels of descriptive detail. The first configuration is the real complete description presented in Table 2. The second configuration corresponds to a simpler design where steel elements between two consecutive reinforced-rubber pipes are not considered for the section between the flange and the second swivel and for the section between the second swivel and the shut-in valve. The third configuration corresponds to the lowest level of detail, where a single long reinforced-rubber pipe is included between the first swivel and the shut-in valve.

The first configuration corresponds to the actual description of the Statfjord offloading system. The second and third configurations correspond to simplified offloading structures and are used to illustrate the contribution of detailed modeling to design and safety in the case of pressure transients.

Before accidental actuation of the shut-in valve, the oil flow in the offloading system was 6000 m^3/h, which corresponded to an 8.2-m/s flowing velocity in a 20-in. pipeline. The flow was fully turbulent, with a Reynolds number of approximately 4.6×10^6. A constant 0.02 steady friction factor was used for modeling of pressure-wave attenuation in the offloading system.

Water hammer in the Statfjord offloading system was simulated using a second-order accurate finite-volume method: namely, the Lax-Wendroff numerical scheme coupled to the Superbee flux limiter (Pierre and Gudmundsson 2009; Laney 1998). Spatial and temporal resolutions were 0.25 and 0.125 milliseconds, respectively. Water hammer was simulated during 4 seconds of propagation that corresponded approximately to the water-hammer travel time between the shutter valve and the pumping station.

Water hammer was simulated for the three offloading-system configurations, using both thin-walled and thick-walled sets of acoustic velocities. Results are compared for the three configurations and the two sets of acoustic velocities in terms of maximum increase in pressure.

Contribution of Accurate Acoustic Velocities

Maximum increases in local pressure in the complete real offloading system for the two sets of acoustic velocities investigated are shown in **Fig. 3.** Calculated maximum increases in pressure are greater on average using the thin-walled set of acoustic velocities than with the thick-walled set of acoustic velocities. Maximum increases in pressure calculated using thin-walled and thick-walled sets of acoustic velocities are on average 48.5 and 45.7 barg, respectively.

Maximum increases in pressure in the real offloading system between the flange and the shut-in valve for the two sets of acoustic velocities investigated are shown in **Fig. 4.** Maximum increases in pressure are greater using the thick-walled set of acoustic velocities than with the thin-walled set of acoustic velocities. Calculated

TABLE 4—ACOUSTIC VELOCITIES				
	d = 0.508 m		*d* = 0.482 m	
	Thin-Walled	Thick-Walled	Thin-Walled	Thick-Walled
Steel	836.6 m/s	809.9 m/s	836.6 m/s	811.2 m/s
Reinforced Rubber	819.1 m/s	458.2 m/s	818.1 m/s	464.3 m/s

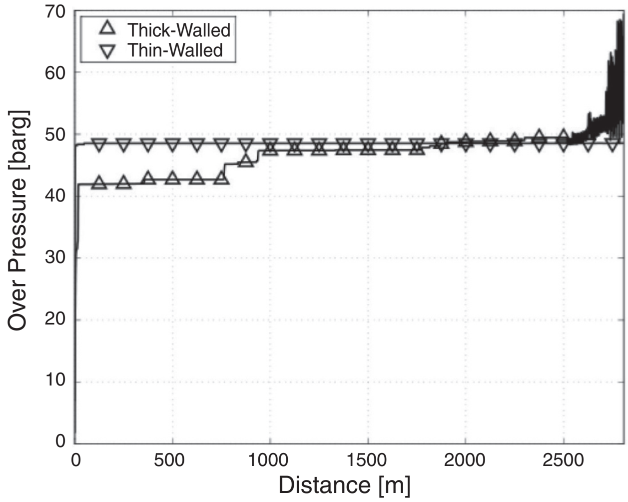

Fig. 3—Maximum increases in pressure in offloading system—thin-walled vs. thick-walled acoustic velocities.

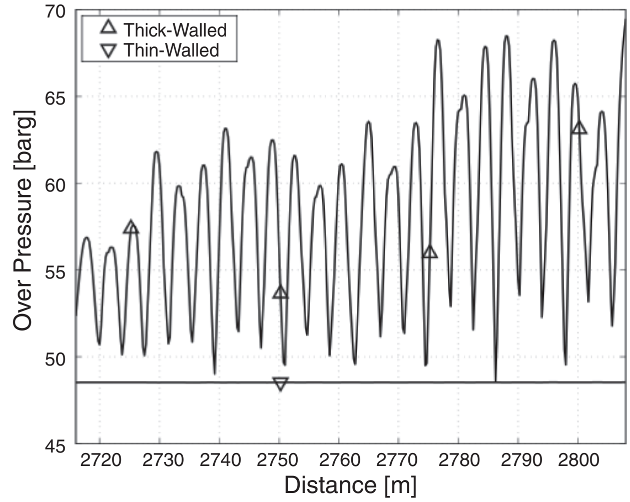

Fig. 4—Maximum increases in pressure between flange and shut-in valve—thin-walled vs. thick-walled acoustic velocities.

maximum increases in pressure using the thick-walled set of acoustic velocities is nearly 69 barg at 2777 m. Oscillations are because of superposition of multiple pressure waves induced at the numerous acoustic interfaces between reinforced-rubber pipes and steel pipes.

The greater the difference between acoustic velocities, the greater the maximum increases in pressure. Another way to express this is that the greater the difference between acoustic velocities, the greater the reflection coefficient, hence the reflected-pressure-wave amplitudes. Superpositions of multiple pressure waves create local pressure peaks, short in time. Thus, oscillations of maximum increases in pressure observed in Fig. 4 for calculations using the thick-walled set of acoustic velocities can be explained by superpositions of multiple pressure waves generated at acoustic interfaces.

Uncertainties related to acoustic velocities in reinforced rubber are related to pipeline-wall Young's modulus of elasticity and to the structure coefficient. Accurate Young's modulus of reinforced-rubber hoses can be measured only experimentally because of the uncertainties related to the steel-reinforcement properties and geometry. Calculated acoustic velocities in reinforced rubber, assuming a Young's modulus of elasticity of 1.9×10^9 Pa, decrease from 819.1 m/s using the thin-walled structure coefficient to 458.2 m/s using the thick-walled structure coefficient. Consequences are a 20-barg difference in maximum increases in pressure between the flange and the shut-in valve.

Realistic values of acoustic velocities are necessary for increasing accuracy in water-hammer calculations. Acoustic velocities can be approximated by calculations, but can also be accurately measured experimentally. Acoustic velocities in reinforced-rubber pipes need particularly to be measured accurately because of the large uncertainty in calculated values.

The greatest difference between acoustic velocities is observed for the thick-walled set of acoustic velocities. The three offloading-system configurations are then to be compared using the thick-walled set of acoustic velocities only.

Contribution of Accurate Offloading-System Description

Maximum increases in pressure using the thick-walled sets of acoustic velocities for the three offloading systems investigated are shown in **Fig. 5.** Maximum increases in pressure are greater on average in the real system than in the two simplified models. Calculated maximum increases in pressure on average are 46.8, 45.3, and 44.9 barg in the real system, the first simplified case, and the second simplified case, respectively.

Maximum increases in pressure between the flange and the shut-in valve, calculated using the thick-walled sets of acoustic velocities for the three configurations investigated, are shown in **Fig. 6.** Calculated maximum increases in pressure are greater in the real configuration than in either of the simplified configurations. The average maximum increase in pressure between the flange and the shut-in valve is approximately 58 barg, with pressure peaks as great as 69 barg at 2777 m.

Oscillations of maximum increases in pressure are because of the multiple superpositions of pressure waves generated at acoustic interfaces between reinforced-rubber pipes and steel pipes. Superpositions of pressure waves induce local pressure peaks that can exceed the original water hammer in amplitude.

The more numerous the acoustic interfaces in an offloading system, the greater the maximum increases in pressure calculated. Thus, from a safety point of view, the more details included in the modeling, the more realistic the calculation.

From a design point of view, the number of changes in pipe properties should be reduced as much as possible. Acoustic interfaces that result from changes in pipe properties generate multiple reflected pressure waves that can lead to local pressure peaks when superimposing.

Recommendations

Modeling results predict maximum overpressures greater than 65 barg between 2770 and 2790 m from the pumping station (Fig. 6). Therefore, modeling results are in good agreement with the location of the actual rupture that took place approximately 2780 m from the pumping station on the Statfjord A offloading system. Therefore, practical recommendations can be drawn directly from the present study, and theoretical recommendations from the modeling.

Theoretical recommendations relate to uncertainties in modeling of acoustic velocity. Of particular importance are the uncertainties in flexible-hose elastic properties, Young's modulus, and Poisson's ratio, because of steel reinforcements. Also, the mathematical definition of acoustic velocity is only an approximation of a physical quantity and more-accurate models need to be developed further (Pierre 2009).

Theoretical recommendations relate secondly to uncertainties in modeling of attenuation of pressure waves. State-of-the-art models are inaccurate and do not represent the physics of the phenomenon (Pierre and Gudmundsson 2009). Overestimating attenuation of pressure waves can lead to pressure peaks greater in amplitude than calculated values, hence potentially damaging the offloading system. Underestimating attenuation of pressure waves establishes a worst-case scenario, but can lead to overdimensioned offloading systems.

Practical recommendations relate first to safety of offloading systems. Of particular importance are accurate details related to

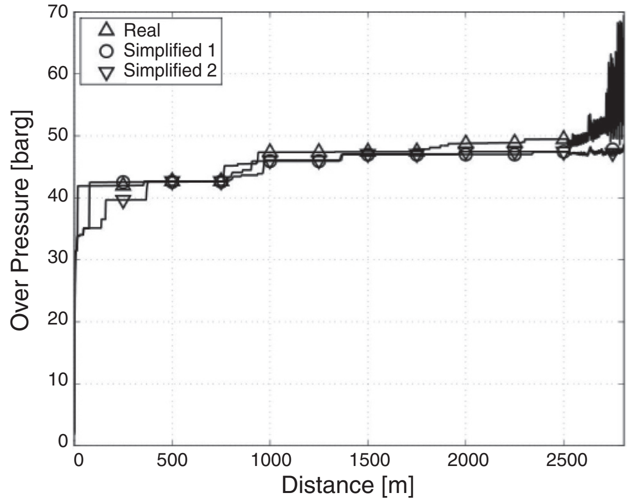

Fig. 5—Comparison of maximum increases in pressure in offloading system.

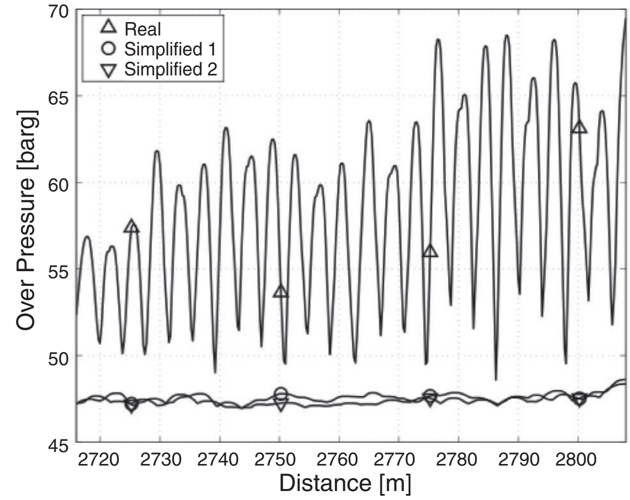

Fig. 6—Comparison of maximum increases in pressure between flange and shut-in valve.

geometry and material properties of each individual pipe that is part of the offloading system because changes in pipe characteristics create acoustic interfaces where pressure waves reflect and transmit, leading further to pressure peaks. The more detailed the modeling of an offloading system, the better the assessment of its safety.

Uncertainties related to pipe material should be reduced by experimentally measuring acoustic velocities in each pipe material that is part of an offloading system. Of particular importance are velocities in flexible hoses where the influence of steel reinforcements is not well established and where the uncertainties about material characteristics are the greatest. Acoustic velocities in steel elements such as flanges should also be measured experimentally for greater accuracy.

Attenuation of pressure waves with distance should also be measured experimentally in each pipe that is part of an offloading system. Theoretical uncertainties about the modeling of water-hammer events in an offloading system can be reduced by experimental investigation of propagation of controlled pressure waves of small amplitudes and known wavelengths, purposefully generated at one end of the system.

Practical recommendations relate secondly to the design of offloading systems. Pressure peaks result from the local and temporal superposition of two or more pressure waves that may be generated by reflections of the initial water-hammer event at acoustic interfaces. The fewer the acoustic interfaces, the fewer the pressure peaks large in amplitude.

Acoustic interfaces result from changes in pipe geometry and material properties. The fewer the pipes that compose an offloading system, the fewer the acoustic interfaces. Another way to express this is that offloading systems should include as few pipe sections as possible, and each pipe should be as long as possible. Because of the flexibility required between the riser and the shut-in valve, offloading systems should include few but long flexible hoses.

Conclusions

- Acoustic velocities need to be measured experimentally for increasing accuracy of water-hammer calculations. Acoustic velocities in reinforced rubber especially need to be measured because of the great uncertainty concerning material elastic properties.
- The more numerous the modeling details, the greater the accuracy in water-hammer calculations; the more detailed the modeling, the better the assessment of pipeline safety.
- The more numerous the changes in pipe properties, the greater the maximum increases in pressure in the offloading system. Offloading systems should include pipes that are as long as possible, to decrease the number of acoustic interfaces responsible for reflections of pressure waves that can lead to local pressure peaks.

Nomenclature

a = acoustic velocity, m/s
d = pipe diameter, m
e = pipe-wall thickness, m
f = steady friction factor
F = external forces, Pa
K_T = fluid isotherm compressibility, Pa^{-1}
p = pressure, Pa
R = reflection coefficient
T = transmission coefficient
u = fluid velocity, m/s
Y = pipe-material Young's modulus of elasticity
z = acoustic impedance, kg/(m^2·s)
μ = pipe-wall-material Poisson's ratio
p = fluid density, kg/m^3
σ_u = structure coefficient

Acknowledgments

The authors want to thank the Norwegian Research Council for providing financial support to Benjamin Pierre, through the Petromaks program, project 196054/S60.

References

Cheremisinoff, N.P. 1996. *Materials Selection Deskbook*. Westwood, New Jersey: Noyes Publications.

Ghidaoui, M.S., Zhao, M., McInnis, D.A., and Ashworthy, D.H. 2005. A Review of Water Hammer Theory and Practice. *Appl. Mech. Rev.* **58** (1): 49–76. http://dx.doi.org/10.1115/1.1828050.

Laney, C.B. 1998. *Computational Gasdynamics*. Cambridge, UK: Cambridge University Press.

McCain, W.D. Jr. 1990. *The Properties of Petroleum Fluids*, second edition. Tulsa, Oklahoma: PennWell Publishing Company.

Misiunas, D., Vitkovsky, J.P., Olsson, G., Simpson, A., and Lambert, M.F. 2005. Pipeline Break Detection Using Pressure Transient Monitoring. *J. Water Resour. Plng. and Mgmt.* **131** (4): 316–321. http://dx.doi.org/10.1061/(ASCE)0733-9496(2005)131:4(316).

Moura, C.H.W., Sampaio, D.S., de Lacerda, I.M., and Selli, M.F. 2004. Monitoring Leakages on Oil Production Offloading at Open Seas Using Statistics Associated With Mass Balance Methods. *Proc.,* ASME Biennial International Pipeline Conference (IPC 2004), Calgary, 4–8 October, Paper IPC04-0763, 2243–2247.

Norwegian Coastal Administration (Kystverket). 2008. Oljeutslipp Statfjord OLS-A 12.12.2007 (in Norwegian). 2008. Investigation report, Activity No. 001037002, Petroleum Safety Authority Norway (PSA), Stavanger, Norway. http://www.ptil.no/getfile.php/PDF/Granskningsrapport.pdf.

Pain, H.J. 1993. *The Physics of Vibrations and Waves*, fourth edition. Hoboken, New Jersey: John Wiley & Sons.

Pierre, B. 2009. Pressure Waves in Pipelines and Impulse Pumping: Physical Principles, Model Development and Numerical Simulations. PhD thesis, Norwegian University of Science and Technology, Trondheim, Norway (December 2009).

Pierre, B. and Gudmundsson, J.S. 2008. Water Hammer Simulation of Pressure in the Failed Flexible Hose for Off-Loading Oil at Statfjord A. Technical Report, Department of Petroleum Engineering and Applied Geophysics, Norwegian University of Science and Technology, Trondheim, Norway.

Pierre, B. and Gudmundsson, J.S. 2009. Modelling of Pressure Wave Propagation in Pipelines: Steady-State and Transient Friction. *Proc.,* Fifth National Conference on Computational Mechanics (MekIT' 09), Trondheim, Norway, 26–27 May, 385–398.

Wang, L., Li, J., Peng, K., Jin, S., and Li, Z. 2004. Petroleum Pipe Leakage Detection and Location Embeded in SCADA. *Proc.,* ASME Biennial International Pipeline Conference (IPC 2004), Calgary, 4–8 October, Vol. 3, 2249–2253.

Watters, G.Z. 1984. *Analysis and Control of Unsteady Flow in Pipelines*. Woburn, Massachusetts: Butterworth-Heinemann.

Wylie, E.B., Streeter, V.L., and Suo, L. 1993. *Fluid Transients in Systems*. Upper Saddle River, New Jersey: Prentice Hall.

Benjamin Pierre is a flow assurance engineer at Intecsea WorleyParsons Group in London. His areas of research interest include processing of oil and gas, transient flows, and multiphase flows. He holds an MEng degree in mechanical engineering from Ecole Nationale Supérieure d'Arts et Métiers Paris, an MSc degree in turbomachinery from University Pierre et Marie Curie Paris VI, and a PhD degree in petroleum engineering from Norwegian University of Science and Technology. He's been an SPE member since 2006 and member of academies in France and the UK. He was the secretary for the SPE Trondheim section from 2007 to 2008. **Jon Steinar Gudmundsson** is professor of petroleum engineering at the Norwegian University of Science and Technology in Trondheim. Gudmundsson worked previously in the Geothermal Divison of the National Energy Authority in Reykjavik, Iceland, and the Department of Petroleum Engineering at Stanford University. He is a Dinstinguished Member of SPE and member of academies in Iceland and Norway.